



Evaluation of the clinical efficacy and safety of modified alveolar cleft bone graft with cone-beam CT digital imaging in children

Yueguang Gu, Chaoting Yan, Zhongyi Yan, Xiaochen Wang, Li Yue, Lei Li

Department of Stomatology, The First People's Hospital of Lianyungang, Lianyungang, China

Contributions: (I) Conception and design: Y Gu; (II) Administrative support: C Yan; (III) Provision of study materials or patients: Z Yan; (IV) Collection and assembly of data: X Wang; (V) Data analysis and interpretation: L Yue, L Li; (VI) Manuscript writing: All authors; (VII) Final approval of manuscript: All authors.

Correspondence to: Yueguang Gu. Department of Stomatology, The First People's Hospital of Lianyungang, No. 182 North Tongguan Road, Lianyungang 222000, China. Email: gu18961325850@163.com.

Background: Cone-beam computed tomography (CBCT) is used to observe the bone density and bone height in children with modified alveolar bone graft (ABG) at different times after operation. In this study, the changes of labial-palatal bone mass in the stable period of bone union and in the bone graft area were investigated to provide reference for subsequent treatment.

Methods: A total of 140 pediatric patients with unilateral complete alveolar cleft were selected and routinely underwent iliac bone grafting. The original data obtained by ProMax 3D (Planmeca) examination were stored in DICOM format at 3 and 6 months postoperatively, and the images were reconstructed by Simplant software (Dentsply Sirona). The bone density of the healthy side was measured at 3 months and 6 months, and the results were expressed as Hounsfield units (HU). The labial and palatal bone height at the bone graft site at 3 and 6 months postoperatively was classified according to the modified Bergland classification method, and was compared with panoramic film classification.

Results: Mean bone density at 3 months after surgery (385.4800 ± 78.39770 HU) was not significantly different from that at 6 months (356.1875 ± 73.67164 HU; $P > 0.05$). There were significant differences between the classification of lip and palatal bone height 3 months after operation and that of the classification of panoramic film in the same month ($P < 0.05$); between the classification of lip and palatal bone height 6 months after surgery compared with that of panoramic film of the same month ($P < 0.05$); and between the classification of bone height degree in labial, palatal, and panoramic slices at 3 months after operation and that at 6 months after operation ($P < 0.05$).

Conclusions: The labial and palatal classification is different, and the bone height classification 6 months after surgery is lower than that 3 months after surgery, indicating the persistence of bone resorption. CBCT can objectively evaluate the bone quality in the bone graft area, which has clinical application value for surgical evaluation value and posttreatment guidance.

Keywords: Alveolar cleft bone grafting; effect of bone graft; CT digital imaging; clinical efficacy

Submitted Apr 07, 2022. Accepted for publication Jul 13, 2022.

doi: 10.21037/tp-22-214

View this article at: <https://dx.doi.org/10.21037/tp-22-214>

Introduction

Second stage bone grafting is the most common method for the treatment of alveolar cleft defect. The purpose of this approach is to reconstruct the alveolar cleft defect and restore the integrity of the maxilla (1). To help the

permanent teeth around the fissure erupt normally, it is essential to provide good bone support for orthodontic treatment and nasolabial deformity rectification, as this can ensure the necessary bone mass required for further implant treatment. Patients with cleft lip and palate must

determine the bone mass in the alveolar process area before orthodontic treatment begins; otherwise, orthodontic treatment will cause permanent damage to the teeth near the alveolar fissure. The time of implantation should not exceed 6–8 months after bone grafting because bone absorption is intensified thereafter (2). Bone integration, the proper function of implants, and the success rate of implantation depend on local healthy bone, sufficient mass of the jaw bone, and the density of the jaw bone. Clinical evaluation of the local bone quality of the mandible before and after dental implantation is of great significance to the success of dental implantation and the recovery of implant recipients. Therefore, the efficacy of alveolar bone grafting must be determined before follow-up treatment so as to select the appropriate timing and method for treatment (3). However, no quantitative study exists concerning postoperative bone mineral density changes, and no reports on bone quality in different time periods have been published thus far. Furthermore, there is no unified standard for the postoperative evaluation of alveolar cleft bone grafting. At present, the efficacy of alveolar process bone grafting is mainly evaluated by 2D images of teeth and alveolar bone, which may include anterior maxillary occlusion film and full-mouth curved surface tomography, which are widely used due to advantages of simplicity, economy, and low radiation (4).

Due to the impact on assessment of the amplification of the irradiation area, angle deviation, overlapping of marker points, and on other areas (5), 2D X-ray film cannot reflect the changes of postoperative bone in all directions of space, and its accuracy and accuracy need to be improved. With the continuous maturity of computed tomography (CT) technology, many researchers have begun to introduce this examination technology into the study of alveolar cleft bone grafting. In some studies, CT scanning was used for the evaluation of alveolar cleft bone grafting. Indeed, many in the field believe that CT examination is more advantageous for observing and measuring bone support in the teeth surrounding the fissure (6). However, the application of conventional CT in the oral cavity is limited by its increased irradiation time and amount as well as the relatively high cost. A cone-beam computed tomography (CBCT) prototype is used for oral clinical application. As a more recent development in CT technology, CBCT provides higher accuracy, faster reconstruction of the bone, and a reduction in the radiometric measurement of patients (7). The noninvasive experimental method is suitable for observing the fine-structure mandibular tissue, and bone

morphology measurement analysis technology is more accurate than is spiral CT (8). Preoperative CBCT was taken to evaluate the bone mass defect. For patients with postoperative 3, 6, 12 months follow-up, shooting CBCT for statistical bone defect area recovery, 12 months after the operation for statistical panoramic films modified alveolar ridge cleft graft surgery success rate, with BERGLAND alveolar ridge cleft graft for statistical classification standard, to crack side bone height and normal side alveolar ridge height ratio for the standard, It can be divided into four types: type I, the height of alveolar bone at the fissure is basically normal; Type II, the height of alveolar bone on the fissure side is at least 3/4 of the height of normal alveolar ridge; In type III, the height of alveolar bone on fissure side is less than 3/4 of normal height. Type IV, no continuous bone bridge at the fracture site. In this criterion, type I and type II are clinically successful; Type III and type IV were clinically failed. The operative success rate of different types of patients and 12 months after operation were analyzed.

Oral cone beam CT is widely used in oral medicine in recent years, it can in the coronal and sagittal and axial position and 3 d images on clear, three-dimensional and intuitively show the MB2 form and direction, can be better found in clinical, MB2, contrast oral panoramic machine, oral cone beam CT can provide three-dimensional image, meet the needs of dental clinical diagnosis and treatment. Conventional alveolar cleft bone grafting has defects such as insufficient palatal bone implant, excessive filling of lip and buccal side, shallow vestibular groove and red lip roll-in. However, it mainly focuses on the influence of various factors on graft resorption after conventional alveolar cleft bone grafting. Quantitative comparison and analysis of bone graft amount and postoperative recovery of modified alveolar cleft bone graft and conventional alveolar cleft bone graft were not conducted. However, the survival ratio of postoperative bone graft amount and postoperative surgical success rate of conventional and modified alveolar cleft bone graft were compared in this study.

In this study, CBCT scanning was performed in patients with unilateral complete alveolar cleft appearing after secondary bone transplantation. The data were directly transferred into Simplant software (Dentsply Sirona) in DICOM format, and the software was used to conduct multiplane reconstruction of the scan data to obtain 3D images of the scan area (9). Simplant software was further used to measure and analyze the bone density and height of the bone graft area at different time periods after bone grafting so as to objectively evaluate the survival of the

bone graft in the operation area (10). The aim of this study was thus to determine objective measures for postoperative orthodontic and implant treatment and to provide a reference for the wider application of CBCT in clinical practice. We present the following article in accordance with the MDAR reporting checklist (available at <https://tp.amegroups.com/article/view/10.21037/tp-22-214/rc>).

Methods

Study participants

From January 2015 to June 2021, a total of 140 children with unilateral complete alveolar cleft were enrolled in the Department of Oral Surgery of our hospital. The study was conducted in accordance with the Declaration of Helsinki (as revised in 2013). The study was approved by the clinical medical ethics committee of The First People's Hospital of Lianyungang (No. LW-20220612001-01). Informed consent was obtained from the patients' parents or legal guardians.

Inclusion criteria

The inclusion criteria for participants were the following: (I) the patient was not accompanied by systemic or other genetic diseases; (II) the diagnosis was unilateral complete alveolar cleft without syndrome, the patient had undergone cleft lip and palate repair and iliac autograft, with orthodontic treatment being performed before surgery; (III) the 3D reconstruction image was clear, with the operation being completed by the same surgeon; and (IV) the participant was between 0 and 12 years of age.

Exclusion criteria

Participants were excluded for any of the following reasons: (I) malignant tumor; (II) severe infection; (III) coagulopathy or diseases of the blood system; and (IV) mental disorder or uncooperative behavior.

Data collection

ProMax 3D software (Planmeca) was used to take 3D images of the bone graft site at 3 and 6 months after surgery. In order to avoid CBCT scanning error, all CBCT scanning (NewTom VGi) of the participants in this study was performed by the same radiologist, the set parameters

and shooting conditions were consistent, and all participants were measured by the same surveyor. SPSS 23.0 software (IBM Corp.) was used to conduct analysis of variance for pairwise comparison between the mean and to compare the mean relative bone mineral density of the 3 measurements. When the significance level of the 3 measurements was 0.05, no significant difference was deemed to be apparent between the 2 measurements, indicating that the results of the 3 measurements had no time correlation and were unaffected by the measurement of the surveyor. In this way, the reliability and reproducibility of the measurement method in this study were ensured (*Table 1*).

Statistical analysis

SPSS 23 statistical software was used for statistical analysis of the following datasets: (I) the healthy side 3 months after surgery; (II) the healthy side 6 months after surgery; (III) bone mineral density at different time points from 3 to 6 months after surgery, with paired *t*-test being used to statistically analyze and calculate the P value. The P value <0.05 was used to determine whether there was a statistical difference between each region and between the two groups (*Tables 2,3*).

Results

Volume of the alveolar ridge fracture defect and area of the alveolar fracture defect

Measurements of the alveolar crest fissure and the basal bone depression of the nasal wing were collected from all patients. Before and 1 year after bone grafting, the volume of the alveolar fracture defect (whole alveolar fracture defect volume) and the alveolar fracture defect area were measured using CBCT with the aid of Mimics software (Materialise). The equipment was adjusted to the patient's natural posture. During the scan, the patients were required to breathe slowly, keep a closed-mouth position, and not clench their teeth or shake. The CBCT parameters included a single 360° rotation, a scanning time of 18 s, and a scanning layer thickness of 0.3 mm. 3D images were stored in DICOM format, and data were imported into Mimics software. For volume measurement, the following steps were performed: DICOM data of the CBCT scans were imported into Mimics software, the alveolar ridge fracture defect area was selected, the threshold and gray value were set, and the 3D model of

Table 1 Bone density measurements

Groups	Uninjured side (HU)	3 months after operation (HU)	6 months after operation (HU)
N1	452.35±107.33	352.35±127.33	321.68±110.33
N2	532.43±89.24	369.88±109.44	339.88±140.35
N3	584.79±104.89	421.59±163.87	395.86±130.57
N4	416.46±89.37	371.81±106.73	396.86±169.89
N5	422.44±107.42	332.44±117.42	321.77±110.41
N6	512.52±89.33	189.79±209.53	239.79±140.84
N7	534.68±104.80	421.68±163.96	395.95±130.66
N8	416.46±89.37	371.81±106.73	396.86±109.89
N9	382.44±107.42	352.44±127.42	321.77±117.42
N10	532.52±89.33	369.99±209.50	339.99±140.14
N11	514.88±104.80	221.68±163.96	195.95±130.66
N12	416.46±89.37	371.81±106.73	396.86±109.89
N13	452.44±107.42	352.44±227.42	321.77±110.42
N14	392.52±89.33	369.79±109.54	339.99±184.45
N15	554.88±104.80	421.68±163.96	395.95±130.66
N16	416.46±89.37	131.81±106.78	126.86±109.89
N17	452.44±107.42	352.44±227.42	321.77±180.42
N18	532.52±89.33	369.99±109.53	339.99±140.44
N19	584.88±104.80	421.68±163.96	395.95±130.56
N20	416.46±89.37	371.81±220.83	396.86±109.89

The data are shown as mean ± SD. HU, Hounsfield unit.

Table 2 *t*-test statistical analysis

Groups	<i>t</i>	P
Uninjured side 3 months after surgery	128.085±88.344	0.001
Uninjured side 6 months after surgery	140.388±90.472	0.001
3–6 months after surgery	11.295±26.055	0.065

The data are shown as mean ± SD.

Table 3 Sample data statistics

Groups	Type	Cases (N)	Mean value	Standard deviation	Standard error of mean
1	Uninjured side	140	475.5750	65.92578	14.81909
	3 months after surgery	140	385.4800	78.39770	17.60790
2	Uninjured side	140	475.5750	65.92578	14.81909
	6 months after surgery	140	356.1875	73.67164	16.55112
3	3 months after surgery	140	385.4800	78.39770	17.60790
	6 months after surgery	140	356.1875	73.67164	16.55112

the preoperative fissure defect area was reconstructed as the typical inverted pyramid shape, with the measured volume referred to as V1 (Figure 1).

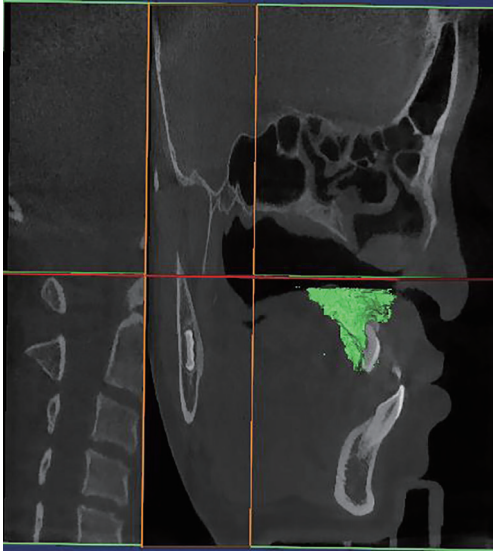


Figure 1 3D model of the preoperative reconstruction of the alveolar ridge cleft defect area of the maxilla. The green part indicates alveolar crest fissure area of maxilla.

Construction of 3D alveolar bone model after bone grafting

The 3D model of the maxillary defect area was reconstructed after surgery, with the measured volume being referred to as V2; thus, the osteogenic volume of the maxillary defect area was calculated as follows: $V_{\text{upper}} = V1 - V2$. The same method was used to reconstruct the 3D model of the alveolar bone before surgery: the reconstruction started from the existing alveolar bone, and the volume of the defect area after reconstruction was denoted as V3. The 3D model of the alveolar bone defect area was reconstructed 1 year after surgery, and the measured volume was referred to as V4; thus, the volume of the alveolar bone defect area was calculated as follows: $\text{Volume (V) tooth} = V3 - V4$ (Figure 2).

Osteogenic effect at 1 year after maxillary and alveolar bone grafting

The percentage of bone formation in the maxillary defect was only 37.75% at 1 year after bone grafting, while that in the alveolar defect was 37.75% after bone grafting, with the percentage of osteogenesis in the final year being 68.69% (Table 4).

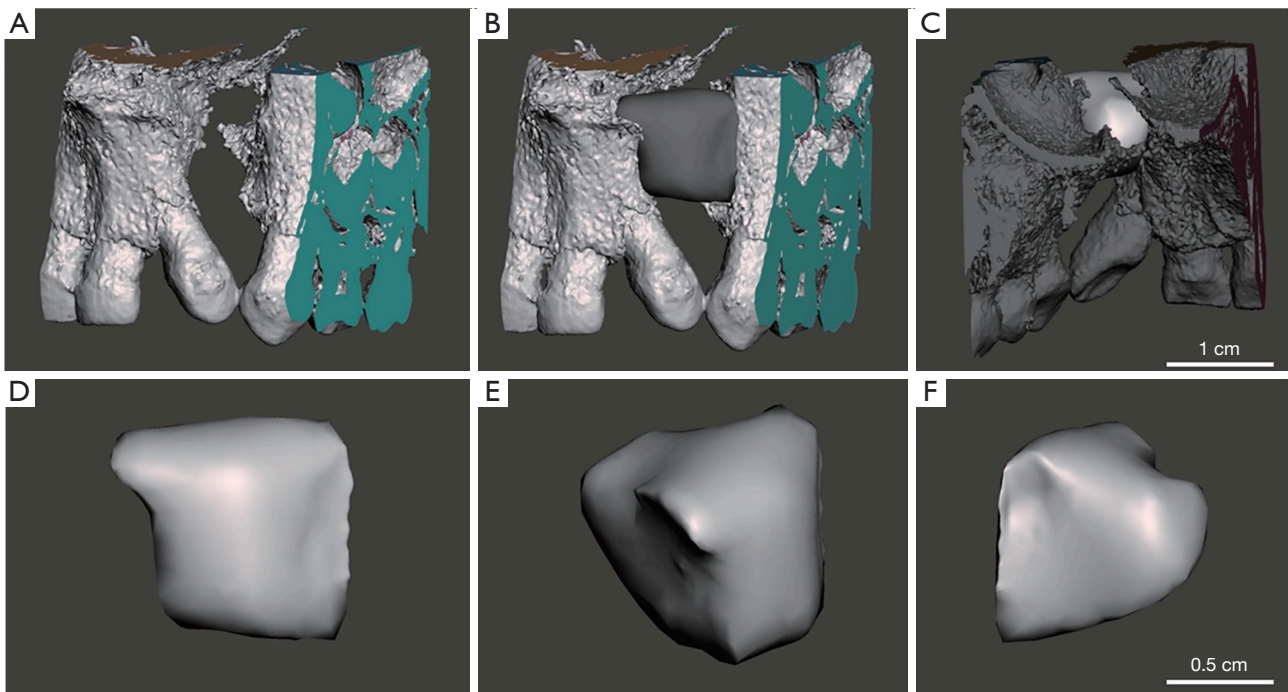
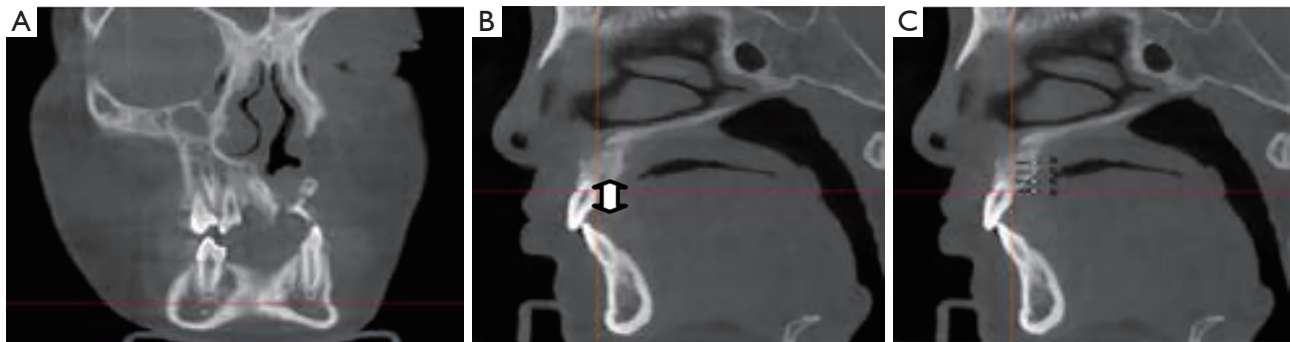


Figure 2 3D model of maxillary defect (A-F).

Table 4 Comparison of the osteogenesis between the maxillary and alveolar bone

Group	Average preoperative defect volume (mm ³)	Average osteogenic volume (mm ³)	Osteogenesis
Maxillofacial bone defect	785.88	360.75	37.75%
Dental alveolar bone defect	345.66	225.45	68.69%

**Figure 3** Conical beam CT measurement (A-C). The arrow indicates Alveolar crest fissure area of maxilla. CT, computed tomography.

Improved Bergland typing evaluation analysis

For vertical alveolar bone height according to the improved Bergland classification, type I was normal alveolar ridge height. In type II, the height of alveolar ridge was more than $\frac{3}{4}$ of the total alveolar height. In type III, the height of alveolar ridge was less than $\frac{3}{4}$ of the total alveolar height. Type IV was a bone bridge without bone implantation in the alveolar cleft space (Figure 3A). The distance from the healthy side of the central incisor and cusp to the crest of alveolar crest (Figure 3B); Labial bone thickness: the alveolar bone thickness 0, 1, 2, and 4 mm from the alveolar crest was measured with the bilateral central teeth and cusp as the target teeth, and was denoted as m 0–4 (Figure 3C).

Discussion

Alveolar fissure bone grafting can fill and repair the gap of alveolar fissures, with the purpose being to rebuild the defect of the alveolar fissure so as to facilitate the emergence of cusp teeth (11). According to the time of bone grafting, alveolar ridge bone grafting can be divided into early stage (before 2 years old), early stage (2–5 years old), second stage (6–15 years old), and late stage (after 16 years old) (12). In this study, 8 patients were late stage II, and the remaining 12 patients were stage II, including 15 patients with tooth malformation extraction and loss

of development in the bone graft area. Most patients require orthodontic and dentition repair immediately after surgery, and shortening the treatment time and improving the appearance of malformation are urgently needed by this patient group (13). Accurate evaluation of the effect of bone grafting can guide clinicians in choosing the timing of treatment (14). Most researchers believe that at 3 months after alveolar fissure bone grafting, the bone healing is basically completed, and the bone structure and alveolar height gradually enter a stable stage. Other studies have shown that the bone tissue healing process in 80% of patients has been stabilized at the bone graft site 6 months after surgery (15–17).

In the pre-experiment of this study, CBCT images of previous patients undergoing postoperative review were preliminarily analyzed (18). The postoperative bone mass of 1 to 2 patients was sufficient, but the initial measurement of bone mineral density was low. Images beyond 12 months postoperatively mostly indicated deficient bone mass. Therefore, this study selected 3 to 6 months after the operation for analysis, and the follow-up time range was controlled within 1 week before and after the operation (19). Bone mineral density reflects bone viability to a certain extent, and the measurement methods are mainly divided into qualitative measurement, semiquantitative measurement, and quantitative measurement. The qualitative measurement of bone mineral density is affected by irradiation dose, irradiation

angle, observer subjectivity, and other factors, and when the mineral loss in bone is less than 30%, it can be difficult to recognize by the naked eye. The method of semiquantitative measurement of bone mineral density is usually expressed by different grades or degrees, which is not accurate and seldom used (20). Quantitative measurement methods mainly include single-photon absorption, two-photon absorption, dual energy X-ray absorption, and quantitative CT, among others. Due to the thin bone mass of alveolar bone, complex surrounding anatomical structure, narrow oral space, and expensive equipment, the application of the above methods in alveolar bone density measurement is limited (21). CT is able to visualize the 3D structure of human tissues. Many researchers have used spiral CT to measure and classify bone mineral density (22). In related studies, Simplant interactive software was used to analyze the mandibular mass in different areas of interest before implantation, and the average CT value of bone around dental implant was used to objectively classify the bone (23). However, the clinical application of conventional CT is limited due to its high radiation exposure and cost. CBCT is suitable for observing the fine structure of the mandibular hard tissue and 3D finite element analysis technology (24). Images obtained by CT scan can be reconstructed by using graphics processing software to observe and measure the images according to different needs (25). But, CBCT alveolar process cleft graft surgery incision of the labial side and the alveolar ridge top remaining mucosa tissue quantity is less, increasing the difficulty of labial side crack closure, and the lateral palatine mucosal is overmuch, easy cause soft tissue accumulation, is not conducive to the edge of healing, easy cause mucosa perforation, influence postoperative effect, and the lateral palatine mucosal surplus too much, often prone to scarring, cause oppression to the bone graft, Bone resorption occurs.

There is no unified standard for postoperative evaluation of modified alveolar cleft bone grafting in children. CBCT observation can be more widely used in future diagnosis and treatment, and the emergence of low-radiation CBCT technology and the development of 3D reconstruction technology and measurement methods will likely raise the standard and quality of alveolar bone graft classification.

Acknowledgments

Funding: None.

Footnote

Reporting Checklist: The authors have completed the MDAR reporting checklist. Available at <https://tp.amegroups.com/article/view/10.21037/tp-22-214/rc>

Data Sharing Statement: Available at <https://tp.amegroups.com/article/view/10.21037/tp-22-214/dss>

Conflicts of Interest: All authors have completed the ICMJE uniform disclosure form (available at <https://tp.amegroups.com/article/view/10.21037/tp-22-214/coif>). The authors have no conflicts of interest to declare.

Ethical Statement: The authors are accountable for all aspects of the work in ensuring that questions related to the accuracy or integrity of any part of the work are appropriately investigated and resolved. The study was conducted in accordance with the Declaration of Helsinki (as revised in 2013). The study was approved by the clinical medical ethics committee of The First People's Hospital of Lianyungang (No. LW-20220612001-01). Informed consent was obtained from the patients' parents or legal guardians.

Open Access Statement: This is an Open Access article distributed in accordance with the Creative Commons Attribution-NonCommercial-NoDerivs 4.0 International License (CC BY-NC-ND 4.0), which permits the non-commercial replication and distribution of the article with the strict proviso that no changes or edits are made and the original work is properly cited (including links to both the formal publication through the relevant DOI and the license). See: <https://creativecommons.org/licenses/by-nc-nd/4.0/>.

References

1. Xu D, Xie C, Yu H, et al. Evaluation of factors affecting alveolar ridge height and facial bone thickness in Chinese maxillary central incisors by cone beam CT. *J Dent Sci* 2021;16:229-35.
2. Sivolella S, Meggiorin S, Ferrarese N, et al. CT-based dentulous mandibular alveolar ridge measurements as predictors of crown-to-implant ratio for short and extra short dental implants. *Sci Rep* 2020;10:16229.
3. Sivolella S, Meggiorin S, Ferrarese N, et al. Publisher Correction: CT-based dentulous mandibular alveolar

- ridge measurements as predictors of crown-to-implant ratio for short and extra short dental implants. *Sci Rep* 2021;11:7370.
4. Şeker BK, Orhan K, Şeker E, et al. Cone Beam CT Evaluation of Maxillary Sinus Floor and Alveolar Crest Anatomy for the Safe Placement of Implants. *Curr Med Imaging* 2020;16:913-20.
 5. Dyakova MV, Bespalova NA, Klochkov AS, et al. Preservation of Bone and Soft Tissue Components of the Alveolar Ridge during Immediate Implantation in the Aesthetic Zone of Jaws with Bone Deficiency. *Sovrem Tekhnologii Med* 2020;12:57-62.
 6. Wen SC, Barootchi S, Huang WX, et al. Time analysis of alveolar ridge preservation using a combination of mineralized bone-plug and dense-polytetrafluoroethylene membrane: A histomorphometric study. *J Periodontol* 2020;91:215-22.
 7. Parvini P, Schwarz F, Hüfner MK, et al. Microstructural volumetric analysis of vertical alveolar ridge augmentation using autogenous tooth roots. *Clin Implant Dent Relat Res* 2020;22:647-53.
 8. Cha JK, Song YW, Park SH, et al. Alveolar ridge preservation in the posterior maxilla reduces vertical dimensional change: A randomized controlled clinical trial. *Clin Oral Implants Res* 2019;30:515-23.
 9. Ma F, Lin Y, Sun F, et al. The impact of autologous concentrated growth factors on the alveolar ridge preservation after posterior tooth extraction: A prospective, randomized controlled clinical trial. *Clin Implant Dent Relat Res* 2021;23:579-92.
 10. Mangano C, Giuliani A, De Tullio I, et al. Case Report: Histological and Histomorphometrical Results of a 3-D Printed Biphasic Calcium Phosphate Ceramic 7 Years After Insertion in a Human Maxillary Alveolar Ridge. *Front Bioeng Biotechnol* 2021;9:614325.
 11. Grassi FR, Grassi R, Vivarelli L, et al. Design Techniques to Optimize the Scaffold Performance: Freeze-dried Bone Custom-made Allografts for Maxillary Alveolar Horizontal Ridge Augmentation. *Materials (Basel)* 2020;13:1393.
 12. Chen ST, Darby I. Alveolar ridge preservation and early implant placement at maxillary central incisor sites: A prospective case series study. *Clin Oral Implants Res* 2020;31:803-13.
 13. Botilde G, Colin PE, González-Martín O, et al. Hard and soft tissue analysis of alveolar ridge preservation in esthetic zone using deproteinized bovine bone mineral and a saddle connective tissue graft: A long-term prospective case series. *Clin Implant Dent Relat Res* 2020;22:387-96.
 14. Zhang Z, Dong Y, Yang J, et al. Effect of socket-shield technique on alveolar ridge soft and hard tissue in dogs. *J Clin Periodontol* 2019;46:256-63.
 15. Wortmann DE, Klein-Nulend J, van Ruijven LJ, et al. Incorporation of anterior iliac crest or calvarial bone grafts in reconstructed atrophied maxillae: A randomized clinical trial with histomorphometric and micro-CT analyses. *Clin Implant Dent Relat Res* 2021;23:492-502.
 16. Virdee S, Tan WC, Hogg JC, et al. Spatial Dependence of CT Emphysema in Chronic Obstructive Pulmonary Disease Quantified by Using Join-Count Statistics. *Radiology* 2021;301:702-9.
 17. Sanchez F, Gutierrez JM, Kha LC, et al. Pathological entities that may affect the lungs and the myocardium. Evaluation with chest CT and cardiac MR. *Clin Imaging* 2021;70:124-35.
 18. Wortmann DE, Klein-Nulend J, van Ruijven LJ, et al. Histomorphometric and micro-CT analyses of calvarial bone grafts used to reconstruct the extremely atrophied maxilla. *Clin Implant Dent Relat Res* 2020;22:593-601.
 19. Costa ED, Peyneau PD, Ambrosano GMB, et al. Influence of cone beam CT volume orientation on alveolar bone measurements in patients with different facial profiles. *Dentomaxillofac Radiol* 2019;48:20180330.
 20. Al-Hafidh NN, Al-Khatib AR, Al-Hafidh NN. Assessment of the cortical bone thickness by CT-scan and its association with orthodontic implant position in a young adult Eastern Mediterranean population: A cross sectional study. *Int Orthod* 2020;18:246-57.
 21. Ramanauskaite A, Becker K, Kassira HC, et al. The dimensions of the facial alveolar bone at tooth sites with local pathologies: a retrospective cone-beam CT analysis. *Clin Oral Investig* 2020;24:1551-60.
 22. Xie L, Li T, Chen J, et al. Cone-beam CT assessment of implant-related anatomy landmarks of the anterior mandible in a Chinese population. *Surg Radiol Anat* 2019;41:927-34.
 23. Xiao L, Pang W, Bi H, et al. Cone beam CT-based measurement of the accessory mental foramina in the Chinese Han population. *Exp Ther Med* 2020;20:1907-16.
 24. Vanderstuyft T, Tarce M, Sanaan B, et al. Inaccuracy of buccal bone thickness estimation on cone-beam CT due to implant blooming: An ex-vivo study. *J Clin Periodontol*

- 2019;46:1134-43.
25. Oda M, Nishida I, Habu M, et al. Imaging peculiarities of gubernaculum tracts in molars as accessional teeth on CT.

Clin Exp Dent Res 2021;7:1205-14.
(English Language Editor: J. Gray)

Cite this article as: Gu Y, Yan C, Yan Z, Wang X, Yue L, Li L. Evaluation of the clinical efficacy and safety of modified alveolar cleft bone graft with cone-beam CT digital imaging in children. *Transl Pediatr* 2022;11(7):1140-1148. doi: 10.21037/tp-22-214